First-Order Transition in the Magnetic Vortex Matter in Superconducting MgB2 Tuned by Disorder

Thierry Klein, R. Marlaud, C. Marcenat, Hervé Cercellier, M. Konczykowski, C. J. van Der Beek, V. Mosser, H. S. Lee, S. I. Lee

First-Order Transition in the Magnetic Vortex Matter in Superconducting MgB_2 Tuned by Disorder

T. Klein,[1,2] R. Marlaud,[1] C. Marcenat,[3] H. Cercellier,[1] M. Konczykowski,[4] C. J. van der Beek,[4] V. Mosser,[5] H. S. Lee,[6] and S. I. Lee[7]

[1]*Institut Néel, CNRS, 25 rue des martyrs, 38042 Grenoble, France*
[2]*Institut Universitaire de France and UJF-Grenoble 1, France*
[3]*SPSMS, UMR-E9001, CEA-INAC/ UJF-Grenoble 1, 17 rue des martyrs, 38054 Grenonle, France*
[4]*Laboratoire des Solides Irradiés, CNRS UMR 7642 & CEA-DSM-IRAMIS, Ecole Polytechnique, 91128 Palaiseau, France*
[5]*ITRON, 76 Avenue Pierre Brossolette, 92240 Malakoff, France*
[6]*NVCRICS and department of Physics, Pohang University of Science and Technology, Pohang 790-784 Republic of Korea*
[7]*NVCRICS and department of Physics, Sogang University, Seoul, 121-742, Republic of Korea*
(Received 18 December 2009; published 19 July 2010)

The field-driven transition from an ordered Bragg glass to a disordered vortex phase in single-crystalline MgB_2 is tuned by an increasing density of point defects, introduced by electron irradiation. The discontinuity observed in magnetization attests to the first-order nature of the transition. The temperature and defect density dependences of the transition field point to vortex pinning mediated by fluctuations in the quasiparticle mean free path, and reveal the mechanism of the transition in the absence of complicating factors such as layeredness or thermal fluctuations.

DOI: 10.1103/PhysRevLett.105.047001 PACS numbers: 74.25.Uv, 74.25.Dw

The nature of the ground state of elastic manifolds pinned by quenched weak disorder has been a central issue in a large variety of systems such as Wigner crystals, charge density waves, magnetic bubble arrays, or vortices in type-II superconductors (see [1] and references therein). It is now well accepted that, for sufficiently weak disorder, the ground state, dubbed the Bragg Glass [1], has long-range orientational order and algebraically decaying positional correlations. Vortices in superconductors rapidly became the system of choice for the study of the influence of disorder on the stability of the Bragg Glass. Namely, the role of disorder can be tuned very easily by changing the external magnetic field H_a. Increasing the field leads to an order-disorder (OD) transition revealed by a peak in the critical current density j_c, that has been the subject of much theoretical work [1–5]. However, no consensus has been reached thus far as to the mechanism of the transition.

In order to experimentally address the issue, we study the vortex lattice in MgB_2. This superconductor is chosen not for its two gap nature, but because it is characterized by a large superfluid density and coherence length ξ_{ab}, and the resulting irrelevance of thermal fluctuations for the vortex phase diagram [6]. Moreover, MgB_2 crystals typically have small critical current densities $j_c \sim 4 \times 10^8$ A m^{-2} (at 4 K and $H_a \rightarrow 0$ [9]) emphasizing the small amount of native disorder. Then, the Bragg Glass should occupy the largest part of the H-T phase diagram. Indeed, as in $NbSe_2$ [10], $j_c(H_a)$ measurements show the existence of a peak effect, i.e., a sudden increase of j_c, but only for H_a close to the upper critical field H_{c2} [11,12].

The peak effect in type-II superconductors was initially attributed by Pippard to the fact that the elastic constants of the vortex lattice vanish more rapidly than the pinning force as $H_a \rightarrow H_{c2}$ [13]. Larkin and Ovchinnikov [14] noted that this is exacerbated by the gradual softening of the vortex lattice because of the nonlocality of its tilt modulus. Kierfeld *et al.* [3] and Mikitik *et al.* [4] contended that the peak occurs at the field H_{OD} at which the pinning energy gained by disordering the vortex ensemble outweighs the energy of elastic deformation due to the generation of edge and screw dislocations. Finally, in Ref. [5], the peak is interpreted as the discontinuous crossover from weak collective pinning to strong pinning.

We show here that the peak effect in MgB_2 overlies a first-order transition of the vortex ensemble. Increasing the defect density in MgB_2 crystals by high energy electron irradiation pushes the transition field rapidly away from H_{c2}. Simultaneously, the initially narrow peak is enhanced, transforming to the so-called ''fishtail effect'' reminiscent of that in cuprate superconductors [15–17]. Both the temperature and defect density dependence of H_{OD} are in very good agreement with the scenario of proliferation of dislocations [4], in conjunction with pinning mediated by fluctuations in the mean free path.

The first-order transition of the vortex ensemble is expected to be accompanied by history effects in magnetization measurements, resulting from phase coexistence [17,18]. Namely, when executing so-called minor hysteresis loops, the local flux density as well as the global magnetic moment depend on the fraction of the ordered and disordered phase present around the transition. History effects similar to those observed in cuprates [18,19] have previously been seen in pristine [12], proton [20], and neutron irradiated [21] MgB_2 crystals. However, clear *thermodynamic* evidence for a first-order phase transition is missing [22]. Here we show that a discontinuity in the reversible magnetization is present in irradiated samples close to H_{OD}, thereby supporting the first-order nature of the transition.

Vortex pinning was characterized by two local magnetization techniques. The ac transmittivity T'_H [23] of the crystals was measured by centering these on a miniature GaAs-based quantum well Hall Sensor (of dimension $8 \times 8\ \mu m^2$). The sensor is used to record the time-varying component B_{ac} of the local induction as the sample is exposed to an ac field of amplitude ~1 Oe and frequency ~210 Hz. The ac transmittivity, T'_H obtained by subtracting the response at 4.2 K from $B_{ac}(T)$ and renormalizing this difference to 1 in the normal state, is directly related to the screening current, $T'_H = 1 - j_c d/h_{ac}$ [23] (with d the sample width). Measurements of the dc "local magnetization" $B - \mu_0 H_a$, were performed by monitoring the local induction, using the same Hall sensor.

Whereas defects with different sizes, from atomic-to-nanometer scale [24,25], are induced by neutron irradiation, low-temperature (20 K) electron irradiation induces only isolated point defects through the formation of Frenkel pairs (the cryogenic irradiation temperature prevents defect clustering and recombination). Therefore, only one single pinning mechanism is expected to characterize our samples, and the low-field j_c is hence a good parameter to characterize vortex lattice order. Four fluences (1.0, 2.2, 2.7, and $5.2 \times 10^{19}\ e^- \mathrm{cm}^{-2}$) were attained in different single crystals from the same batch. No significant change in T_c or in the transition width [deduced from $T'_H(T)$ in zero magnetic field] could be observed. Note that our values of T_c (~35–36 K) are slightly lower than the optimal value (~38–39 K) probably due to small chemical inhomogeneity, not affecting the conclusions drawn here. Furthermore, $H_{c2}(4.2\ \mathrm{K})$ for $H_a \parallel c$, determined as the field at which T'_H reaches 1, remained ~3.3 T for fluences up to $2.7 \times 10^{19}\ e^- \mathrm{cm}^{-2}$ [Fig. 1(a)]. It went up to 4.6 T for $5.2 \times 10^{19}\ e^- \mathrm{cm}^{-2}$, suggesting that this latter sample is not in the clean limit anymore.

Figure 1(a) shows that irradiation leads to a dramatic change in the field dependence of T'_H. Indeed, as observed in other artificially disordered samples [20,21,24] the small drop in T'_H related to the increase of j_c close to H_{c2} in the pristine sample, is enormously enhanced and pushed away from the $H_{c2}(T)$ line (see Fig. 2) once point defects are introduced. Above a characteristic field H_{onset}, T'_H now rapidly drops to zero, signaling the restoration of full screening over a wide field range. In contrast to the curve for the pristine crystal, $T'_H(H_a)$ shows marked hysteresis: screening on the descending field branch is much stronger than on the ascending field branch. This effect attests to the presence of the disordered state (with high j_c) at fields where it is not in equilibrium. Similarly, the inset to Fig. 2 shows that the increase of j_c responsible for the drop in T'_H at H_{onset} corresponds to a pronounced "fishtail effect" of the local magnetization hysteresis loops. Moreover, $B - \mu_0 H_a$ on the descending field branch of the loops depends on the value of the field at which the ramp direction has been reversed, reflecting the progressive transformation of the vortex ensemble from the low-field to the high-field state as the field is increased. The effect, very similar to that observed in [18,19] (see also [21]), attests to phase separation, and to a nucleation-propagation type transition.

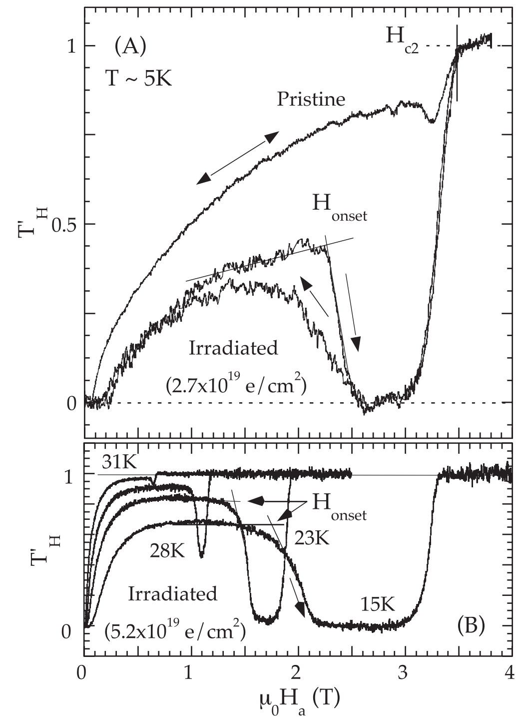

FIG. 1. (a) Field dependence of the ac transmittivity in a pristine, and in an irradiated MgB_2 single crystal ($2.7 \times 10^{19}\ e^- \mathrm{cm}^{-2}$). Note the hysteresis between increasing and decreasing field branches for $H_a \sim H_{onset}$ after irradiation. (b) Transmittivity of a crystal irradiated to $5.2 \times 10^{19}\ e^- \mathrm{cm}^{-2}$, at the indicated temperatures (ascending field branch only).

As in proton- [20] and neutron- [21,24] irradiated samples, the large value of the irreversible magnetization close to H_{onset} prevents any reliable determination of the reversible contribution in crystals having undergone irradiation fluences exceeding $2.7 \times 10^{19}\ e^- \mathrm{cm}^{-2}$. However, in crystals having received a lower dose, the hysteresis can be nearly suppressed by application of the vortex equilibration or "shaking" technique [26] [see Fig. 3(b)]. Both the ascending—and descending field branches then show an upward shift for $H_a \sim H_{onset}$, revealing a step in the reversible part of the flux density. This step becomes more apparent after subtraction of a smooth background (dotted line) from the reversible part of the magnetization, defined as $M_{rev} = \frac{1}{2}(B_{up} + B_{down}) - \mu_0 H_a$ [Fig. 3(a)]. The step in the local flux density is also observed in the field-cooled

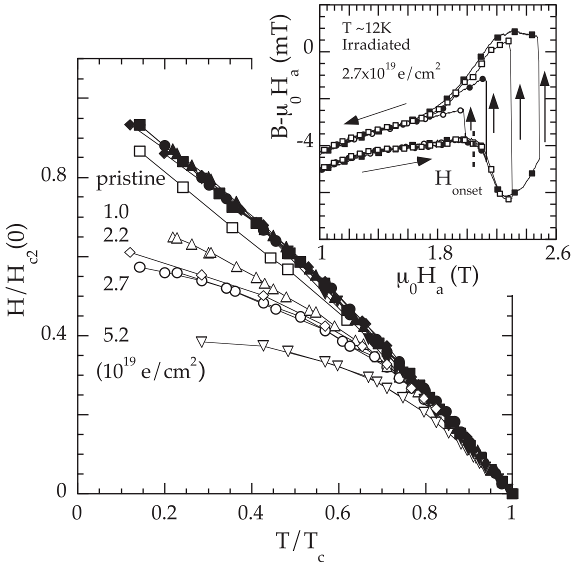

FIG. 2. (H_a, T) phase diagram of vortex matter in electron-irradiated MgB_2. The H_{c2} line (closed symbols) is identified as the field at which T'_H reaches unity (see Fig. 1). Open symbols correspond to the peak effect field $H_{\rm onset}$, determined from T'_H (Fig. 1) and from local magnetization curves (inset). The inset also shows the influence of the maximum field attained on the decreasing branch of the magnetization curve, as one cycles through minor loops [same crystal as Fig. 1(b)].

magnetization [Fig. 3(c)], its position coincides with $H_{\rm onset}$ deduced from T'_H.

We now shift our attention to the evolution of the vortex matter phase diagram as a function of the point defect density. Figure 2 shows the temperature dependences of H_{c2} and $H_{\rm onset}(T)$ for all fluences. In neutron-irradiated samples, the fishtail effect has been associated with the presence of large defects [21,24]. We show here that the first-order transition at $H_{\rm onset}$ is also progressively pushed away from the $H_{c2}(T)$ line as the *point* defect density is increased. Note that, as pointed out by Pissas *et al.* [12] in pristine samples, the peak becomes unmeasurable above a temperature T^* that is progressively shifted towards T_c for increasing defect density, reaching $\sim 0.94 T_c$ for irradiation with $5.1 \times 10^{19}\ e^- {\rm cm}^{-2}$.

In spite of the widely varying values of $h_{\rm OD}(0) \equiv H_{\rm OD}(0)/H_{c2}(0)$ one can show that the mechanism for the peak effect is the same, and corresponds to the proliferation of a dislocation network in the vortex lattice [3,4]. To set the stage, note that just below $H_{\rm onset}$, the $j_c(5\ {\rm K})$ values ($\sim 10^6\ {\rm A\,m^{-2}}$ in pristine samples and $10^7\ {\rm A\,m^{-2}}$ after irradiation with $2.7 \times 10^{19}\ e^-/{\rm cm}^2$) correspond to translational correlation lengths [14] R_c largely exceeding the penetration depth [$R_c \sim 20\ \mu$m and $10\ \mu$m respectively, while $\lambda_{\rm ab} \approx 500$ nm], which means that nonlocality of the elastic constants, and the scenario of Ref. [14] can be disregarded. As stated in the introduction, thermal fluctuations, quantified by the Ginzburg number $\mathrm{Gi} \equiv \frac{1}{2}[k_B T_c/\varepsilon\varepsilon_0\xi_{\rm ab}]^2 \sim 10^{-6}$ [with $\varepsilon_0 = (\Phi_0/4\pi\lambda_{\rm ab})^2$ and ε the coherence length anisotropy ~ 0.2] can also be fully neglected. $H_{\rm OD}$ can then be calculated by equating the gain $E_{\rm pin}$ in pinning energy with the cost $E_{\rm el}$ in elastic energy associated with the proliferation of dislocations [4]. Writing $E_{\rm el} \sim 4\sqrt{\pi} c_L^2 (c_{44}c_{66})^{1/2} a_0^3$ and $E_{\rm pin} \sim (f_{\rm pin}^2 n_d (c_{44}/c_{66})^{1/2} a_0^3)^{1/2}\xi$, with $f_{\rm pin}^2$ the average of the square of the pinning force, a_0^{-2} the vortex density, n_d the defect density, $h_{\rm OD}(T)$ should be given by

$$h_{\rm OD}(1 - h_{\rm OD})^3 = \frac{1}{2\pi c_L^8}\left[\frac{g(T) j_c^{\rm SV}(0)}{j_0(0)}\right]^3. \tag{1}$$

Here we used $c_{66} \approx (\varepsilon_0/4a_0^2)(1-h)^2$ and $c_{44} \approx (\varepsilon^2\varepsilon_0/a_0^2)(1-h)$ for the shear and tilt modulus, respectively, $h \equiv H_a/H_{c2}(T)$, and c_L as the Lindemann number. The critical current density in the single vortex limit $j_c^{\rm SV} = j_0(\varepsilon\xi/L_c)^2$ and L_c, the *single vortex* collective pinning length, are direct measures of the disorder strength, while j_0 is the depairing current ($\approx 10^{12}\ {\rm A\,m^{-2}}$ in MgB_2 for $T \to 0$). $g(T)$ is a temperature-dependent function that depends on the pinning mechanism (δl vs δT_c- pinning, see below). As shown in Fig. 4, plotting $h_{\rm onset}^{1/3}(1 - h_{\rm onset})$ as a function on $h_{c2}(T)$ leads to a collapse of all transition curves onto

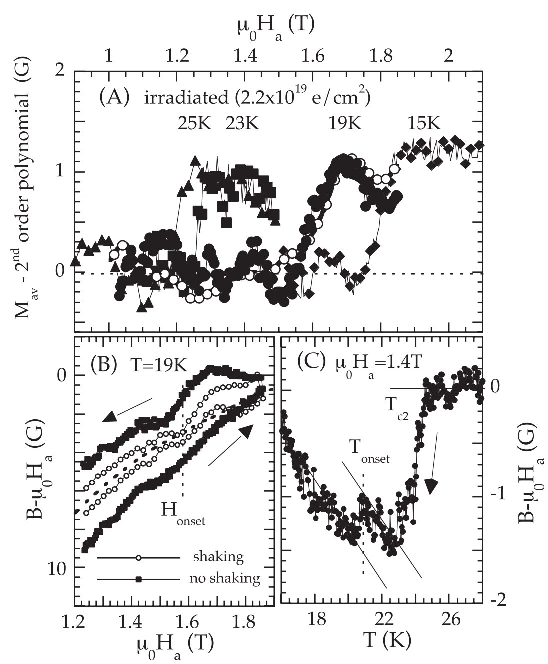

FIG. 3. (a) Step in the reversible part of the local magnetization $M_{\rm rev} = \frac{1}{2}(B_{\rm up} + B_{\rm down}) - H_a$ of the crystal irradiated with $2.2 \times 10^{19}\ e^-\ {\rm cm}^{-2}$, after subtraction of the smooth background depicted by the dotted line in Fig. 4b. Closed (open) symbols represent measurements performed with (without) ac shaking. (b) Local magnetization in the vicinity of the peak onset at 19 K, measured with (○) or without (●) a 20 Oe ac equilibration field. (c) Field-cooled magnetization (in $\mu_0 H_a = 1.4$ T), showing a small step at $T_{\rm onset} \sim 20.5$ K.

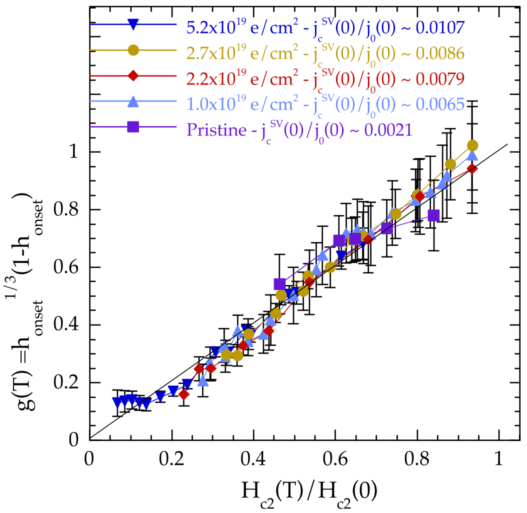

FIG. 4 (color online). Temperature dependence of $g(T) = h_{\text{onset}}^{1/3}(1 - h_{\text{onset}})$ ($h_{\text{onset}}(T) = H_{\text{onset}}(T)/H_{c2}(T)$) deduced from the transition lines of Fig. 2 using Eq. (1), plotted as a function of $H_{c2}(T)/H_{c2}(0)$. Corresponding $j_c^{\text{SV}}(0)/j_0(0)$ [see Eq. (1)] values (taking $c_L = 0.2$) are given in the legend.

each other as expected from Eq. (1). Moreover, one obtains that $g(T) \propto H_{c2}(T)/H_{c2}(0)$ as predicted for pinning induced by fluctuations in the mean free path [4,5]. δT_c pinning would lead to $g(T) \propto [H_{c2}(T)/H_{c2}(0)]^{-1/3}$, in utter disagreement with the experimental data. In spite of the fact that the large defects induced by neutron irradiation do not lead to weak collective pinning [21,27], and that the peak effect occurs in the presence of both strong—and weak pinning contributions to j_c, similar conclusions as to δl pinning have been reached in [21,24].

Note that, deviations from Eq. (1) may occur in MgB_2 for very large irradiation doses (i.e., small H_{OD} values) due to the influence of H_a on the two gaps [24]. However, in our case, H_{OD} lies well above the field for which the small gap is suppressed [28] and MgB_2 behaves here as a single (σ) band system. Finally, note that $j_c^{\text{SV}}(0)$ (see legend of Fig. 4 for values) well agrees with the expected $j_c^{\text{SV}} \propto 1/L_c^2 \propto n_d^{2/3}$ behavior, if one takes a defect density proportional to the electron dose. The corresponding $j_c^{\text{SV}}(0)$ values are in fair agreement with the experimental j_c for $H_a \rightarrow 0$ ($\approx 4 \times 10^8$ and $\approx 1 \times 10^9$ A m^{-2} for pristine and the most irradiated samples, respectively).

In conclusion, the discontinuity in the equilibrium flux density accompanying the critical current peak effect in electron-irradiated single-crystalline MgB_2, and the marked history dependence of the irreversible magnetization, strongly support the presence of a first-order phase transition. The evolution of the transition field with temperature and defect density testifies that the phase transition from the well ordered Bragg glass to the disordered phase is mediated by the proliferation of edge and screw dislocations, while vortex pinning is through the δl mechanism [4].

[1] T. Giamarchi and P. Le Doussal, Phys. Rev. B **55**, 6577 (1997).
[2] T. Nattermann and S. Scheidl, Adv. Phys. **49**, 607 (2000).
[3] J. Kierfeld and V. M. Vinokur, Phys. Rev. B **61**, R14 928 (2000); **69**, 024501 (2004).
[4] G. Mikitik and E. H. Brandt, Phys. Rev. B **64**, 184514 (2001); Phys. Rev. B **68**, 054509 (2003); Phys. Rev. B **71**, 012510 (2005).
[5] G. Blatter, V. B. Geshkenbein, and J. A. Koopman, Phys. Rev. Lett. **92**, 067009 (2004).
[6] The relative importance of fluctuations in MgB_2 is 2 orders of magnitude smaller than in (K, Ba)BiO_3 [7], and more than 4 orders of magnitude smaller than in NdFeAs(O,F) [8].
[7] S. Blanchard *et al.*, Phys. Rev. Lett. **88**, 177201 (2002); I. Joumard *et al.*, Phys. Rev. Lett. **82**, 4930 (1999).
[8] J. Kacmarcik *et al.*, Phys. Rev. B **80**, 014515 (2009), and references therein.
[9] C. U. Jung *et al.*, Phys. Rev. B **66**, 184519 (2002).
[10] S. Bhattacharya and M. J. Higgins, Phys. Rev. Lett. **70**, 2617 (1993); Y. Paltiel *et al.*, Nature (London) **403**, 398 (2000).
[11] H. J. Kim *et al.*, Phys. Rev. B **71**, 174516 (2005).
[12] M. Pissas *et al.*, Physica (Amsterdam) **456C**, 153 (2007).
[13] A. B. Pippard, Philos. Mag. **19**, 217 (1969).
[14] A. I. Larkin and Y. N. Ovchinnikov, J. Low Temp. Phys. **34**, 409 (1979).
[15] M. Daeumling, J. M. Seuntjens, and D. C. Larbalestier, Nature (London) **346**, 332 (1990).
[16] N. Chikumoto *et al.*, Phys. Rev. Lett. **69**, 1260 (1992).
[17] C. J. van der Beek *et al.*, Phys. Rev. Lett. **84**, 4196 (2000).
[18] A. P. Rassau *et al.*, Physica (Amsterdam) **328C**, 14 (1999).
[19] S. Kokkaliaris *et al.*, Phys. Rev. Lett. **82**, 5116 (1999).
[20] J. D. Moore *et al.*, Phys. Rev. B **71**, 224509 (2005).
[21] M. Zehetmayer *et al.*, Phys. Rev. B **69**, 054510 (2004).
[22] An anomaly in the *field derivative* of the magnetic torque has been reported by T. Nojima *et al.*, J. Phys. Conf. Ser. **150**, 052189 (2009), but without any clear evidence of a discontinuity of the magnetization itself.
[23] J. Gilchrist and M. Konczykowski, Physica C (Amsterdam) **212**, 43 (1993).
[24] M. Zehetmayer *et al.*, Supercond. Sci. Technol. **20**, S247 (2007).
[25] A. Martinelli *et al.*, Supercond. Sci. Technol. **21**, 012001 (2008).
[26] M. Willemin *et al.*, Phys. Rev. Lett. **81**, 4236 (1998).
[27] The superposition of different kinds of defects in proton irradiated samples may also explain deviations for the temperature dependence of the order-disorder line mentioned in [20].
[28] Z. Pribulova *et al.*, Phys. Rev. Lett. **98**, 137001 (2007).